Morphology and Phase Behavior of Blends of a Styrenic Block Copolymer Ionomer and Poly(caprolactone)

Xinya Lu and R. A. Weiss*

Polymer Science Program and Department of Chemical Engineering, University of Connecticut, Storrs, Connecticut 06269-3136

Received January 19, 1993; Revised Manuscript Received April 1, 1993

ABSTRACT: The morphology and phase behavior of blends of a lightly sulfonated styrenic block copolymer ionomer and poly(caprolactone) (PCL) were investigated by small-angle X-ray scattering and differential scanning calorimetry. Miscibility of PCL in the ionomeric microphase was enhanced due to exothermic interactions between the sulfonate groups and the polyester. In the blends, PCL exhibited unique crystallization behavior due to the effects of miscibility and the restriction imposed by the microdomains. The addition of PCL also changed the microstructure of the block copolymer from a less ordered, elongated spherical morphology to a well-defined lamellar arrangement.

Introduction

The ordered microstructure and phase behavior of mixtures containing a block copolymer and a homopolymer are of considerable contemporary interest.[1-7] The addition of a homopolymer that is miscible with one of the block segments can dramatically change the microstructures and properties of the block copolymer. Because of the poor thermodynamic miscibility of most polymer pairs, however, the choice of miscible homopolymers to blend with block copolymers is limited. Most previous studies have involved homopolymers having repeat units identical with one of the blocks of the block copolymers, e.g., blends of polystyrene with a styrenic block copolymer[4,5] or polybutadiene with a styrene–butadiene di- or triblock copolymer.[2] Relatively few studies have considered blends where the homopolymer is different from either of the segments of the block copolymer but still miscible with one of blocks.[8-10]

One important difference between a homopolymer (HP)/block copolymer (BC) blend and a HP/HP blend is that there is always a solubility limit of HP in the microdomains of a BC, even when the corresponding HP/HP blend is completely miscible at all compositions. Theoretical and experimental investigations have shown that the solubility limit is a strong function of the molecular weight ratio (M_H/M_B) of homopolymer (M_H) and the block segment (M_B). For example, for an athermal blend of polystyrene HP and a styrenic block copolymer, high solubility requires that $M_H/M_B \leq 1$. The question considered in the present paper is whether this restriction holds in systems where specific interactions occur between the HP and the BC. That is, in strongly interacting systems, is it possible to achieve a high level of solubility even when M_H/M_B is substantially larger than unity?

Miscibility of polystyrene homopolymer (PS) with many heteroatom polymers can be significantly enhanced by incorporating relatively small amounts of sulfonic acid or metal sulfonate groups into PS.[11-13] That result suggests that the miscibility of heteroatom polymers with the polystyrene block (b-PS) of a styrenic block copolymer may be achieved by lightly sulfonating the b-PS. Such sulfonated styrenic block copolymers were recently reported by our laboratory.[14] One of the most important advantages of using a sulfonated PS (or b-PS) in a blend is that the nature and strength of the specific interactions with another HP can be adjusted by the choice of the sulfonation level and/or the choice of the cation.[15] This fact presents opportunities for a broad examination of specific interaction effects on the microdomain structure and solubility limit of BC/HP blends, as well as for improving the properties of BC's by incorporation of miscible HP's.

It is well established that miscibility in HP/HP blends is usually due to exothermic interactions between the two polymers. In a HP/BC blend, the relationship between solubility and specific interactions is more complicated, through one expects *a priori* that the solubility of the HP in a block of the BC should increase with increasing strength of the specific interactions for a given molecular weight ratio M_H/M_B.

Blends involving crystallizable components are also of considerable practical interest. Many studies of crystallization behavior in HP/HP blends have been reported in the past several decades.[16-19] For a miscible blend, the crystallinity and melting point decrease as the concentration of the noncrystallizable component increases. The crystallization behavior of crystalline–amorphous block copolymers has also been investigated.[20-23] Compared with the corresponding HP/HP blend, the melting point for a crystallizable segment of a BC usually exhibits a larger decrease due to the size restriction presented by the microdomains of the block copolymer. A second question probed in the present paper is how is the crystallization of a crystallizable HP affected by blending it with an amorphous BC. Little knowledge about this aspect of HP/BC blends is available in the literature. Both the BC microstructure and the solubility of the HP in the domains of a BC should influence the crystallization behavior, which is likely to be different from that in a HP/HP blend or in a neat block copolymer with a crystallizable block.

In this paper, we describe blends of a semicrystalline HP, poly(caprolactone) (PCL), with a lightly sulfonated styrene/ethylenebutylene/styrene triblock copolymer (SSEBS). This system was chosen to address the two questions raised in the preceding paragraphs: (1) lightly sulfonated PS (SPS) is totally miscible with PCL over the sulfonation range from ca. 5 to 13 mol % and (2) PCL is a crystallizable polymer, so studies of its blends with SSEBS will provide an insight into how a restricted geometry, i.e., the BC microdomains, affects the crystallization behavior of PCL. Studies of blends of SSEBS and PCL will reveal how the microstructure of a BC affects miscibility when strong intermolecular interactions occur between those components. In this blend system, a

0024-9297/93/2226-3615$04.00/0 © 1993 American Chemical Society

complicated morphology is anticipated because of microphase separation of the BC and crystallization of PCL. Small-angle X-ray scattering (SAXS) was used to characterize the morphology of the blends, and the phase behavior and crystallization of the blends were investigated by differential scanning calorimetry (DSC).

Experimental Section

Materials. The sulfonated styrene/ethylenebutylene/styrene triblock copolymer was prepared by sulfonating a hydrogenated poly(styrene/butadiene/styrene) triblock copolymer, Kraton 1652, obtained from Shell Development Co. After hydrogenation, the midblock was essentially a random copolymer of ethylene and butylene. The SEBS had an M_n = 50 000 and a composition of 29.8 wt % styrene. The sulfonation procedure has been described elsewhere.[14] The sulfonation level of the SSEBS was determined to be 8.3 mol % by titration of the acid form of the functionalized copolymer in a toluene/methanol (90/10, v/v) solution with methanolic sodium hydroxide (NaOH).

Sulfonated polystyrene (SPS) was prepared in a similar manner, following the procedure described by Makowski et al.[24] The starting PS was a commercial product of Dow Chemical Co., Styron 666, and had an M_n = 106 000 and M_w = 288 000, as determined by gel permeation chromatography. The sulfonation level was determined by titration of SPS in a toluene/methanol solution with methanolic NaOH.

PCL with an M_w = 40 000 was purchased from Polysciences Inc.

Blend Preparation. SSEBS (sulfonic acid derivative) and PCL were dissolved in the desired proportions in a common mixed solvent of toluene/methanol (95/5, v/v) to produce a 5% (w/v) blend solution. Films were cast from solution in air at room temperature and then dried to constant weight under vacuum. Blends of SPS and PCL were also prepared by mixing in solution; however, because the solubility of SPS in toluene was poor, it was first dissolved in tetrahydrofuran (THF) and then diluted with toluene to achieve a 50/50 (v/v) mixture of the two solvents. A solution of the PCL in toluene was added dropwise to a stirred SPS solution. Films of the blends were cast from solution at ca. 75 °C, which is above the melting point of the PCL, so that the miscibility of the blends could be assessed by the film transparency without the complication of PCL crystallinity.

Differential Scanning Calorimetry. Thermal analyses of the blends were carried out with a Perkin-Elmer DSC 7 using a heating rate of 20 °C/min. The glass transition temperature (T_g) was defined as the midpoint of the change in the specific heat, and the melting point (T_m) was taken as the maximum of the melting endotherm. The effect of thermal history on the crystallization behavior and melting point of the blends was examined by employing various cooling and heating rates between 2.5 and 40 °C/min.

Small-Angle X-ray Scattering. Small-angle X-ray scattering (SAXS) experiments were performed on the SUNY X3A2 Beamline at the National Synchrotron Light Source, Brookhaven National Laboratory. The data were collected with a linear position-sensitive detector with a usable length of 4.5 cm. The sample-to-detector distance and X-ray wavelength were 132 cm and 0.154 nm, respectively. These conditions give a measurable scattering vector, q = 0.06–1.2 nm^{-1}, where $q = (4\pi/\lambda)\sin\theta$, λ is the X-ray wavelength and 2θ is the scattering angle. All the data were corrected for detector sensitivity, parasitic and background scattering, and sample absorption. The background correction factor was determined by fitting the high-q region according to the theory of Porod.[26]

Results and Discussion

Miscibility of SPS and PCL. It is instructive to first consider the miscibility of SPS and PCL, because this will provide a useful reference for assessing the miscibility of SSEBS and PCL. Miscibility of SPS and PCL was investigated in the sulfonation range of 1–23 mol %. The

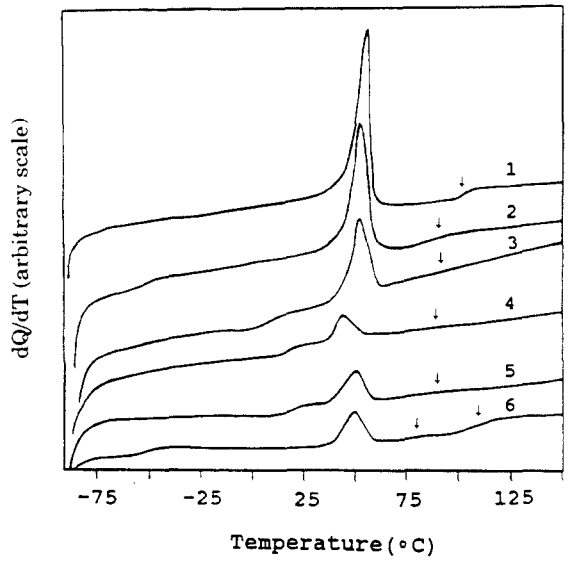

Figure 1. DSC thermograms of 50/50 SPS/PCL blends as a function of sulfonation level: (1) 0, (2) 3, (3) 5, (4) 8, (5) 13, (6) 16 mol % sulfonation. The glass transition temperatures are indicated by the arrows.

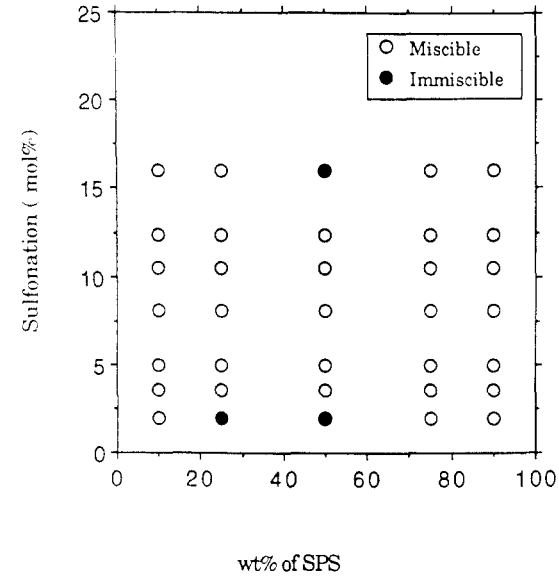

Figure 2. Miscibility of SPS/PCL blends as a function of composition and sulfonation level.

criteria used here for miscibility were optical clarity above the T_m of the PCL and a single, composition-dependent T_g.

Figure 1 shows the DSC thermograms of 50/50 (w/w) SPS (sulfonic acid derivative)/PCL blends as a function of the sulfonation level. PS was immiscible with PCL, as is evident by the observation of two T_g's that corresponded to those of the two constituent polymers and the opacity of the melt above T_m of the PCL. Over a sulfonation range of 5–13 mol %, the SPS/PCL blends were miscible, as indicated by a single T_g and by the transparency of the melts. Below 5% and above 13% sulfonation, the blends were partially miscible; i.e., they exhibited two T_g's, but those were shifted to higher and lower temperatures than the respective T_g's of PCL and SPS. Miscibility of SPS with PCL also resulted in a depression of T_m and a large reduction in the crystallinity.

Figure 2 shows a miscibility diagram for the SPS/PCL system as a function of the blend composition and the sulfonation level. The optimum condition for miscibility was at ca. 8 mol % sulfonation, which was the midpoint of the miscibility window. This was the sulfonation target

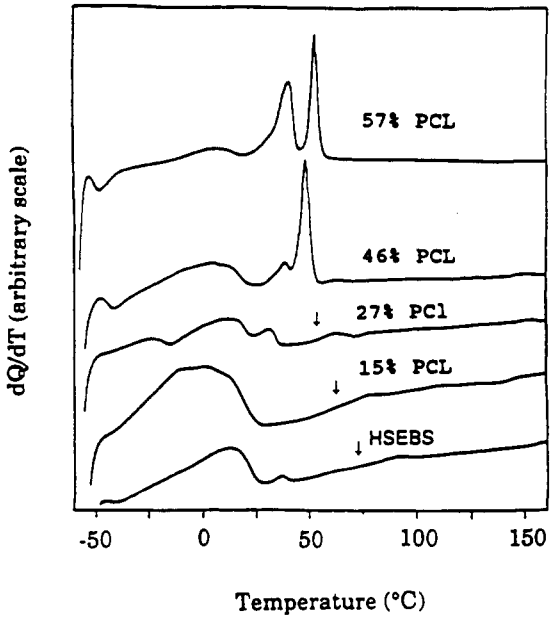

Figure 3. DSC thermograms of SSEBS/PCL blends as a function of composition between 0 and 57% PCL. The glass transition temperatures of the b-SPS/PCL phase are indicated by the arrows.

chosen for studying the PCL/SSEBS blend, though the actual sulfonation level of the SSEBS was 8.3 mol %.

Miscibility of SSEBS and PCL. The neat SSEBS had a microphase-separated microstructure that consisted of a rubbery continuous phase of poly(ethylene-*co*-butylene) and hard microdomains of block SPS (b-SPS). The rubbery block had a T_g at ca. −40 °C, and the b-SPS had a broad glass transition centered at ca. 79 °C. The broadening of the T_g of the b-SPS was probably due to a distribution of domain sizes resulting from imperfect formation of the self-assembled microstructure. Figure 3 shows the DSC thermograms for the 8.3-SSEBS/PCL blends containing 0, 15, 27, 46, and 57% (by weight) PCL based on the mass of the b-SPS phase. A very broad endotherm between ca. −20 and +20 °C is probably due to melting of very small crystallites formed by long sequences of ethylene.

The addition of 15% PCL to the SSEBS lowered the T_g of the hard phase from ca. 79 °C to ca. 58 °C but had no influence on the T_g of the rubbery phase. This indicates that the PCL dissolved only in the b-SPS microdomains. Increasing the PCL concentration to 27% decreased the T_g of the hard phase to ca. 54 °C, and a very weak endotherm also appeared at 31 °C. This small endotherm was most probably due to crystallization of the PCL that occurred in the solution-cast blend even though the PCL concentration was relatively low. Because T_m was ca. 30 °C lower than that of the neat PCL, the crystallites formed in this blend must have been very small and imperfect. This suggests that the PCL crystallized within the restricted geometry of the SPS microdomain, as will be shown by the SAXS data discussed later in this paper. That is, the growth of the PCL crystallites was constrained by the size of the microdomains, which was on the order of 20–30 nm. Cast films containing 15% and 27% PCL were optically transparent, which is an additional indication that all the PCL was contained within the microdomain; i.e., the size of the domain was too small to scatter visible light.

At higher PCL concentrations, the T_g of the hard phase was no longer resolved because of the interference of melting endotherms that occurred in the same temperature region. For 57% PCL, two endotherms were observed at 45.5 and 58 °C, respectively. There are two possible origins of the two endotherms: (1) they correspond to two different populations of PCL crystallites, e.g., inside and outside the b-SPS microdomains, or (2) they result from premelting, followed by recrystallization and remelting, which is often observed in homopolymers or HP/HP blends. As will be discussed later in this paper, the first explanation is believed to be the correct one, and these results indicate that the solubility limit of PCL in the b-SPS microdomains is ca. 46% PCL. Above that concentration, PCL phase separates from the block copolymer.

The solubility limit of a HP in the ordered microdomains of a BC is expected to depend on the molecular weight ratio of the HP and the appropriate block of the BC (M_H/M_B), any specific interactions between the HP and the BC, the microstructure geometry, and temperature. Various thermodynamic theories[1,3] predict the solubility behavior of a homopolymer in a block copolymer, but those theories only consider athermal mixtures where the HP is chemically identical to one block of the copolymer. For example, Meier[1] predicted that significant solubility of a HP in a BC occurs only when $M_H/M_B \leq 1$. If the BC microstructure is lamellar and the $M_H/M_B = 1$, the maximum solubility of homopolymer A in the A phase of an AB or ABA block copolymer is predicted to be ca. 14%.

The solution-cast SSEBS/PCL blend had a lamellar microstructure as determined by SAXS and a molecular weight ratio, $M_H/M_B \sim 5.3$, far in excess of unity. Nevertheless, the DSC data indicate that the solubility limit within the b-SPS was ca. 46% PCL, which is much higher than predicted by the available theories.[1,3] This is not totally unexpected, since those theories do not consider the effects of strong enthalpic interactions. For the PCL/SSEBS blends, hydrogen bonding between the sulfonic acid groups of the b-SPS and the ester groups of the PCL is possible, and, on the basis of the results for this system, one may postulate that the solubility limit for an HP/BC blend increases as the magnitude of the interactions increases.

Melting Behavior of SSEBS/PCL Blends. Figure 4 shows the heating thermograms of the SSEBS/PCL blends cast from solution. The melting temperatures and melting enthalpies as a function of composition are summarized in Table I. As expected, blending PCL with the SSEBS significantly affected the melting behavior of the PCL; see Figure 4. A single endotherm at ca. 65 °C was observed for the neat PCL, but multiple endotherms were observed for all the blends containing ≥57% PCL. Even when the blend contained only 3% of the SPS block, this multiple melting behavior was seen, but the details of the multiple melting endotherms varied with the blend composition. With increasing PCL concentration, the higher temperature endotherm, hereafter referred to as the α-endotherm, increased in intensity relative to the lower temperature endotherm, the β-endotherm. In the literature, different explanations have been advanced to account for multiple melting behavior. Multiple melting endotherms may stem from concurrent melting and recrystallization,[26] which is the case in many homopolymers or miscible HP/HP blends crystallized from the melt. On the other hand, multiple melting endotherms can also result from a complex sample morphology, e.g., when a polymer crystallizes in different phases in a multiphase system. This may have been the case for the PCL/SSEBS blends, which certainly have a complex microstructure. The origin of the multiple melting in the SSEBS/PCL

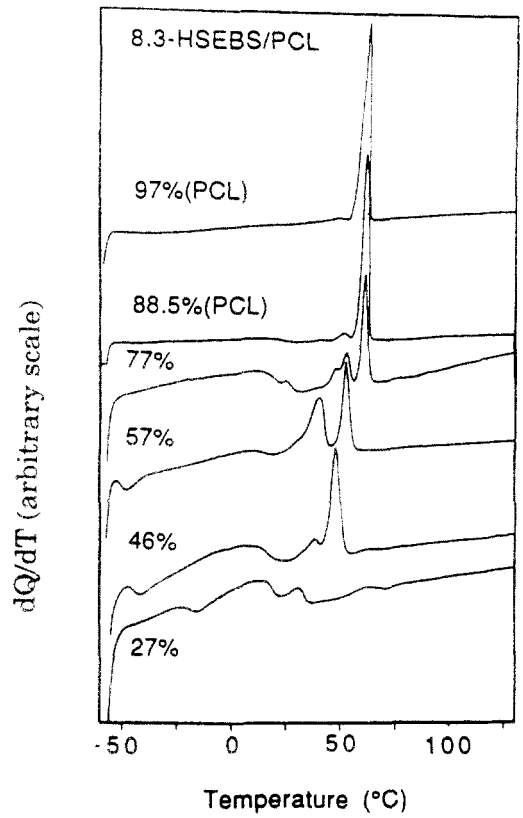

Figure 4. DSC thermograms of SSEBS/PCL blends as a function of composition between 27 and 97% PCL.

Table I. DSC Melting Point Data for Solution-Cast PCL/SSEBS Blends

sample	$T_{m,\alpha}$ (°C)	$\Delta H_{m,\alpha}$ (J/g)	$T_{m,\beta}$ (°C)	$\Delta H_{m,\beta}$ (J/g)
100% PCL	63.0			
97% PCL	62.8	98.3	48.8	4.5
89% PCL	62.3	38.1	52.5	3.8
77% PCL	62.5	16.5	53.0	3.1
57% PCL	58.0	8.9	45.5	13.5
46% PCL			42.6	7.7
27% PCL			31.0	0.8

blends is of particular interest, since the composition dependency of the multiple melting endotherms may provide information about the miscibility of the PCL in the sulfonated styrene microdomains.

The origin of the multiple melting endotherms in these blends was resolved by using variable-rate heating and cooling DSC studies. Figure 5 shows the effect of the heating rate on the melting behavior of a solution-cast blend of 57% PCL. If the double endotherm were due to premelting/recrystallization/melting of the PCL, resolution of two separate endotherms should disappear as the heating rate is increased. Instead, the separation between the α- and β-endotherms was relatively insensitive to heating rate, which indicates two separate thermal events were occurring. The shifts in the peaks in Figure 5 were due to inertial effects that affect the temperature calibration of the instrument; the temperatures in Figure 5 were not corrected for this. This result indicates that the α-endotherm and β-endotherms must be due to different PCL morphologies, and the most likely explanation for this is that distinctly different crystallite sizes existed within the b-SPS microdomains and in a separate PCL phase within the rubbery matrix.

The crystallization of the PCL should also be sensitive to its environment. If there were only one environment, e.g., if all the PCL were in the b-SPS microdomains, there should be only one distinguishable crystallization exotherm

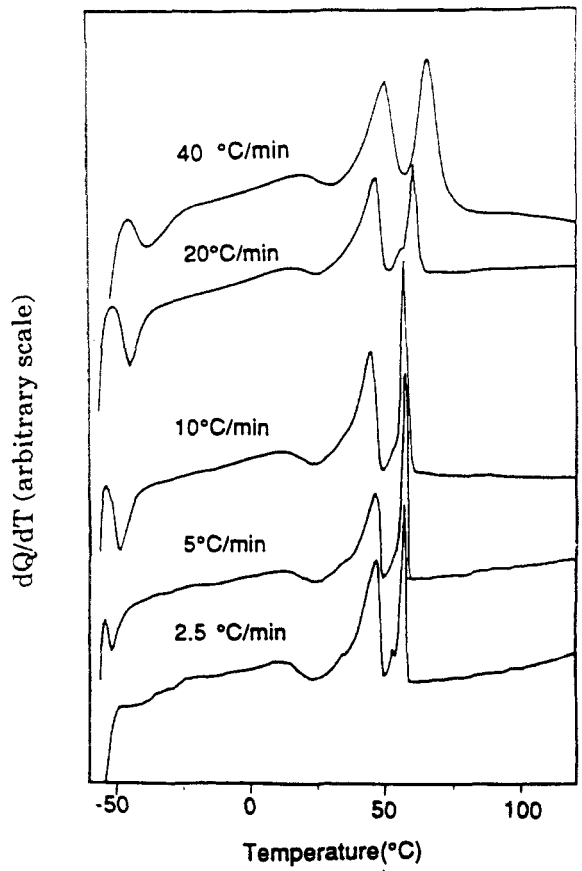

Figure 5. Effect of heating rate on the melting behavior of a 43% SSEBS/57% PCL blend.

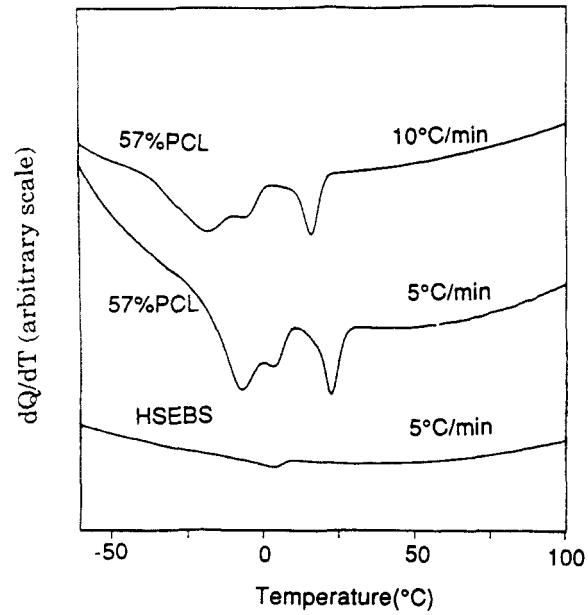

Figure 6. Effect of cooling rate on the crystallization behavior of the neat SSEBS and a 43% SSEBS/57% PCL blend.

when the sample was cooled in the DSC. Alternatively, if there are multiple environments of the PCL, multiple crystallization exotherms are possible. Therefore, the DSC cooling scans of the blends should also distinguish between the two explanations for the origin of the multiple melting endotherms. Figure 6 shows the cooling thermograms of the 57% PCL blend for two different cooling rates and a cooling thermogram for the neat SSEBS. Three exotherms were observed in each cooling scan for the blend, and the cooling rate affected only the transition temperatures, which was a kinetic effect, and not the relative positions of the peaks. The middle exotherm at ~10 °C was due

to a small amount of crystallization of the rubbery block of the BC, as evident by a similar exotherm in the neat SSEBS. The other two exotherms are presumed to correspond to the two PCL melting endotherms observed in the heating scans for the blends. This result is consistent with the conclusion made in the preceding paragraph that there are two different environments for the PCL. The composition of the phase should affect the crystallization temperature of the PC, and, on this basis, we assigned the higher temperature exotherm to a separate, PCL macrophase and the lower temperature exotherm to crystallization of PCL within the b-SPS microdomains. In the latter case, the depression of the crystallization temperature was probably due to the strong intermolecular interactions between the two polymers, which also led to enhanced miscibility of the PCL in the b-SPS, and the small crystallite size required in the b-SPS microdomains. The change of the appearance of the films from transparent to translucent when the PCL content exceeded 46% also indicates the formation of a dispersed phase large enough to scatter light, i.e., μm-sized PCL crystallites.

Since the occurrence of multiple melting endotherms results from phase separation of the PCL from the b-SPS microdomains, the variation of the melting behavior with blend composition provides a useful way to estimate the solubility limit of the PCL in the b-SPS. As shown in Figure 4, the α-endotherm, characteristic of the phase separation of PCL from the b-SPS microdomains, is absent until the PCL concentration reaches 46%, while the β-endotherm, indicative of the crystallization within the microdomain, is clearly present in the 57% PCL blend. From the observed melting behavior of the blends, the maximum solubility of PCL in the b-SPS was estimated to be ~46% PCL.

The value of T_m can also provide useful information about miscibility and morphology of a blend. T_m of a miscible blend is expected to decrease with the addition of the noncrystallizable component because of both morphological effects[27] and thermodynamic effects.[28] As shown in Figure 4, the melting temperature of the α-endotherm was nearly independent of composition, especially when the PCL concentration was ≥77%. This again suggests that the α-endotherm represents a nearly pure PCL phase.

The observation of premelting followed by recrystallization and remelting in a DSC heating scan is still possible if a sufficiently low heating rate is employed. For example, when a heating rate of 2.5 °C/min was used, two very weak endotherms occurred on the lower temperature sides of the α-endotherm and β-endotherm (Figure 5). These two events, which were not resolved at higher heating rates, may very well have been due to the premelting of the PCL.

The conclusion that the double endotherm was due to different PCL morphologies was further assessed by examining the effect of annealing temperature on the DSC thermograms. Figure 7 shows the melting behavior as a function of annealing temperature for a blend with 57% PCL. In order to eliminate any influence of the sample history, the sample was heated to 70 °C, held there for 5 min, then quenched to the annealing temperature, and held for 30 min. When the sample was annealed at 20 °C, the α- and β-endotherms were too close to be clearly resolved. When the annealing temperature was increased to 25 °C, however, four endotherms (denoted β_2, β, α, and α_2 in order of increasing temperature) were observed in the subsequent heating thermogram. Both the α- and β-endotherms shifted to higher temperature and separated

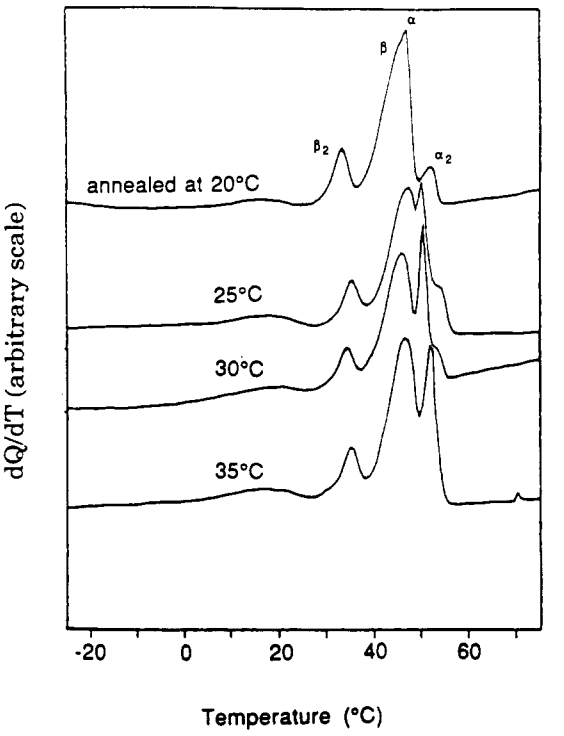

Figure 7. Effect of annealing temperature on the melting behavior of a 43% SSEBS/57% PCL blend.

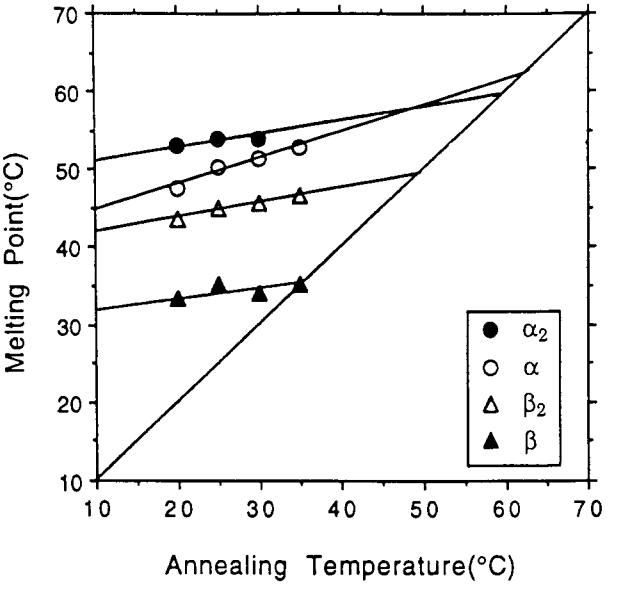

Figure 8. Hoffman–Weeks plot for a 43% SSEBS/57% PCL blend.

with respect to each other as the annealing temperature increased. The differences in the effect of annealing temperature on the two endotherms further confirmed that they arose from two different morphologies. When the blend was annealed at 35 °C, the α_2-endotherm was no longer observed. The four melting peaks are plotted as a function of the annealing temperature in Figure 8. Neither the α_2-endotherm nor the β_2-endotherm was particularly sensitive to the annealing temperature, which suggests that these events originated with the cooling or reheating of the blend and not with annealing. The α- and β-endotherms, however, increased linearly with annealing temperature. Following the method of Hoffman and Weeks,[29] equilibrium melting points corresponding to the α- and β-endotherms were calculated to be 64.1 and 49.2 °C, respectively. The former value is very close to the T_m of pure PCL (63.5 °C), which is not unexpected if

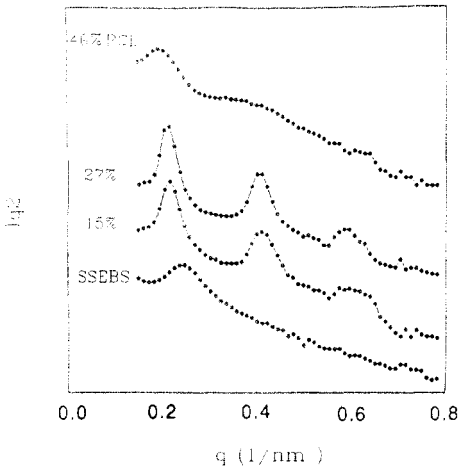

Figure 9. Lorentz-corrected SAXS profiles for SSEBS and SSEBS/PCL blends.

as discussed earlier this event arises from phase separation of a fairly pure PCL phase.

Microstructure of SSEBS/PCL Blends. Small-angle X-ray scattering (SAXS) patterns of the blends containing 0–46% PCL are shows in Figure 9. The neat SSEBS exhibited only a broad SAXS peak at ca. $q = 0.251$ nm^{-1}. The absence of higher order SAXS maxima and transmission electron microscopy images of the BC microstructure[30] indicated that the neat SSEBS possessed a poorly ordered microstructure, probably due to the strong ionic associations within the SPS blocks that prevent that block from self-assembly. After the addition of 15% PCL, however, two higher order scattering maxima were resolved. The positions of those peaks in q-space corresponded to a ratio of 1:2:3, which is indicative of a well-defined lamellar microstructure. Increasing the PCL concentration to 27% resulted in further resolution of the higher order scattering peaks.

The microstructure variation with the addition of PCL to SSEBS can be understood from both kinetic and thermodynamic considerations. First, miscibility of PCL with the b-SPS hard phase significantly lowered the hard-phase T_g and also disrupted the ionic associations within the b-SPS phase. This increased the mobility of the component blocks and facilitated formation of a well-ordered microstructure. Second, swelling the b-SPS phase with PCL increased the volume fraction of the hard phase sufficiently to make a lamellar microstructure more thermodynamically favorable. Finally, since the electron density of the PCL (0.596 mol electron/cm^3) is higher than that of the b-SPS (0.575 mol electron/cm^3), the addition of the PCL to the b-SPS hard phase enhanced the electron contrast between the hard phase and rubbery phase (0.486 mol electron/cm^3), which increased the SAXS intensity.

When the PCL concentration was increased to 46%, the microstructure of the blend became less ordered, as evidenced by the loss of resolution in the SAXS pattern in Figure 9. Although the first three maxima were detected, indicating that the microstructure remained lamellar, the peaks were severely broadened. This indicates significant concentration fluctuations were present within the microdomains. As shown by DSC (Figure 4), at this composition a portion of the PCL crystallized within the b-SPS microdomains, which was very likely responsible for the broadening of the SAXS peaks in Figure 9. Because of the volume restrictions posed by the b-SPS microdomains, the PCL crystallites formed within them must be very small, which is consistent with the low T_m that was measured by DSC. No new peaks corresponding to a long spacing for PCL crystallites were observed by SAXS. The real space range covered by these SAXS measurements was ca. 2–30 nm. It is highly unlikely that there could be a long spacing for the PCL crystallites of less than 2 nm, and it is also impossible for the long spacing to exceed the thickness of the BC lamellae, which was ca. 25–30 nm. Therefore, any scattering due to the long spacing of PCL crystallites in the microdomains must have occurred within the q-range used here. Since the long spacing of the PCL crystallites must be controlled by the BC microstructure, a distribution of lamellar thicknesses and long spacings would explain the broadening of the SAXS patterns shown in Figure 9.

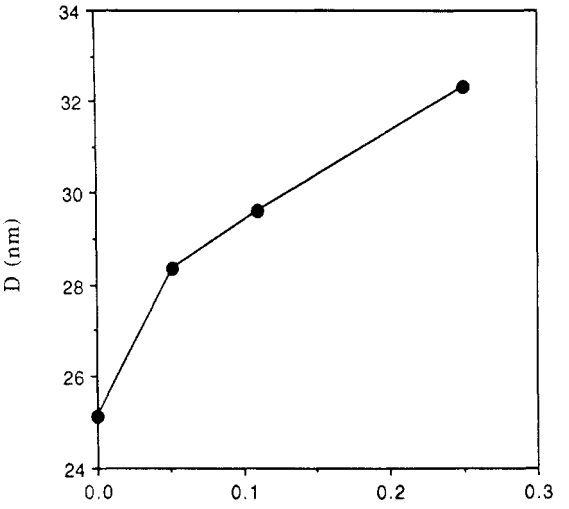

Figure 10. Average nearest-neighbor distance of the microdomains for the SSEBS/PCL blends.

The first-order scattering peak in Figure 9 is related to the average nearest-neighbor distance D between the BC microdomains by the following equation:

$$D = 2\pi/q_m \quad (1)$$

where q_m is the position of the first-order scattering maximum. If the lamellar microstructure persists and the EB lamellar thickness does not change appreciably upon the addition of PCL D is related to the PCL concentration by[30]

$$D = D_s\{1 + (V_S/V_{PCL})[W_{PCL}/(1 - W_{PCL})]\} \quad (2)$$

where D_s is the average nearest-neighbor distance in the neat SSEBS, V_S and V_{PCL} are the specific volumes of SSEBS and PCL, respectively, and the mass fraction of PCL, W_{PCL}, is based on the total mass of the hard and soft phases. According to eq 2, a plot of D vs $[W_{PCL}/(1 - W_{PCL})]$ should give a straight line if the lamellar microstructure and miscibility of the blend are independent of PCL content. D is plotted against $W_{PCL}/(1 - W_{PCL})$ in Figure 10. The linearity of the data for the blends containing 15–47% PCL indicates that, over this concentration range, PCL was miscible with the b-SPS microdomains and the blends have similar lamellar microstructures. The experimental D for the neat SSEBS, however, was lower than that determined from a linear extrapolation of the data for the blends using eq 2. This may be a consequence of a nonlamellar morphology of the neat SEBS. The reason for this may be that the microstructure in neat SSEBS was not lamellar; transmission electron microscopy (not shown) indicated that the actual microstructure was intermediate between spherical and cylindrical.[31]

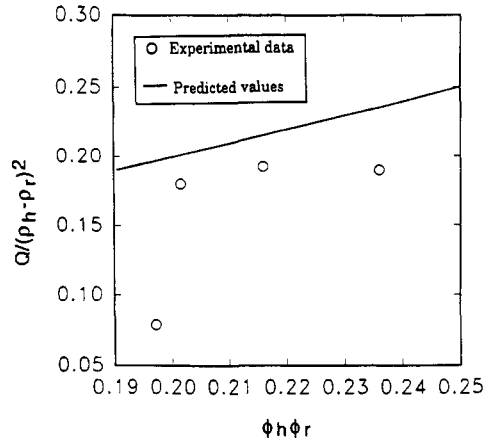

Figure 11. Comparison of experimental and predicted values of $Q/(\rho_h - \rho_r)^2$ as a function of $\phi_h\phi_r$ for SSEBS/PCL blends.

Additional information about the microphase separation of the SSEBS/PCL blends can be determined from the scattering invariant, Q, of the system. For a two-phase system with a sharp interface, the scattering invariant is directly related to the volume fraction of the microdomains by

$$Q = \int q^2 I(q)\, dq = V(\rho_h - \rho_r)^2 \phi_h \phi_r^2 \qquad (3)$$

where V, ρ, and ϕ are the total scattering volume, the electron density, and the volume fraction of the phases. The subscripts h and r refer to the hard phase (b-SPS) and rubbery phase (EB block), respectively. Since $(\rho_h - \rho_r)^2$ and $\phi_h\phi_r$ (when $\phi_h < 0.5$) will increase by the addition of PCL, eq 3 predicts that Q should increase if the PCL is contained within the b-SPS microdomains.

The experimental $Q/(\phi_h - \phi_r)^2$ vs $\phi_h\phi_r$ are compared with the prediction of eq 3 in Figure 11. For the neat SSEBS, the Q calculated from the SAXS pattern is almost 60% lower than the value predicted by eq 3. Such a low Q reflects a poorly ordered microstructure with possibly a broad interphase. As explained earlier, the poorly defined microstructure might be a consequence of the strong ionic associations that occur in the b-SPS hard phase. Studies of SPS ionomers showed that ionic aggregation is stable in these materials even at elevated temperatures.[32] When the SSEBS was cast from the solution, it is possible that the ionic aggregation of the b-SPS formed before the microdomains of the block copolymer were able to self-organize. The experimental Q increased substantially with the addition of 15% and 27% PCL, through the Q calculated from the SAXS pattern was still a little lower than the prediction of the two-phase model (Figure 11). This indicates that the microstructures formed in these blends were much more ordered than the neat SSEBS. The lower than predicted value for the experimental Q suggests that the interface of the microdomains was not particularly sharp. When the PCL concentration was increased to 46%, the discrepancy between the experimental and predicted Q's increased, which may be indicative of a broader interphase region in that sample.

Conclusions

The miscibility of poly(caprolactone) in a styrenic block copolymer was significantly enhanced by partial sulfonation of the styrenic block. Although the molecular weight of the PCL was much higher than that of the sulfonated polystyrene block, the miscibility limit of PCL in the sulfonated polystyrene block of a block copolymer with a sulfonation level of 8.3 mol % was 46%. This miscibility

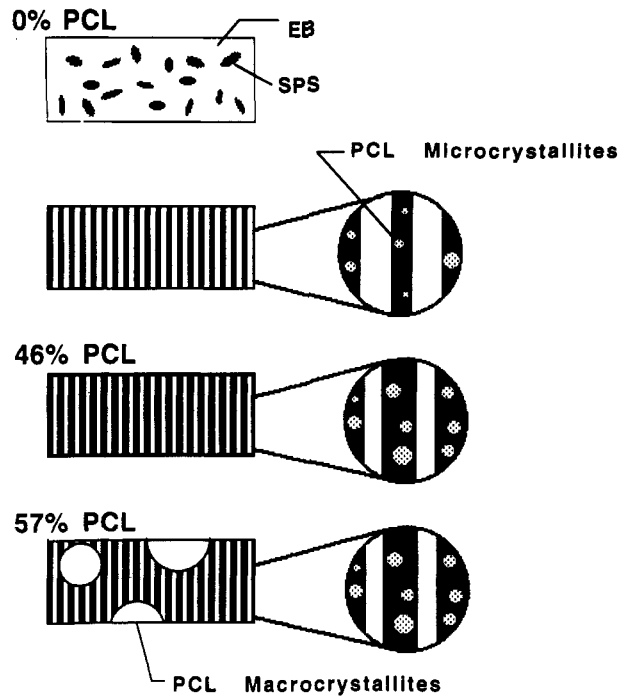

Figure 12. Schematic illustration of the morphology of SSEBS/PCL blends as a function of PCL concentration (*not drawn to scale*).

greatly exceeded the predictions of several contemporary theories, and the enhanced miscibility is believed to be due to exothermic interactions between the sulfonated groups and the poly(caprolactone).

Figure 12 is a proposed schematic description of the variation of the SSEBS/PCL morphology with changing composition. When the PCL concentration was lower than 27%, the PCL was completely miscible with the b-SPS microdomains and the blends exhibited a lamellar BC microstructure. Upon the addition of more PCL, some of the PCL crystallized within the b-SPS microdomains and formed small nanometer-sized PCL crystallites as a consequence of the space constraint imposed by the microdomains. These melted at a temperature ca. 20 °C lower than that of pure PCL. Macrophase separation of the PCL from the microdomains occurred when the PCL concentration ≥46%, and a separate, pure PCL phase was formed, dispersed within the rubbery phase. In that case, two different PCL crystallites coexisted: (1) nanometer-sized crystallites within the b-SPS microdomains and (2) larger crystallites typical of a distinct PCL phase.

The addition of PCL affected the ordered microstructure in the blends. The neat SSEBS had a poorly ordered morphology intermediate between a spherical and cylindrical microstructure, probably because the ionic association within the SPS blocks made it more difficult to develop an ordered microstructure. The addition of 15% PCL to the SSEBS resulted in a well-defined lamellar microstructure, and increasing the PCL concentration to 27% further refined that morphology.

Acknowledgment. We gratefully acknowledge support of this research by the Office of Naval Research (Grant N00014-91-J-1565). We also thank Dr. Carl Willis of Shell Development Co. for providing the starting SEBS block copolymer and Dr. Benjamin Hsaio for his help with the SAX experiments. Time on the SUNY Beamline at Brookhaven National Laboratory, which is supported by the Department of Energy, was kindly provided by Prof. Benjamin Chu.

References and Notes

(1) Meier, D. J. *Polym. Prepr. (Am. Chem. Soc., Div. Polym. Chem.)* **1977**, *18* (1), 340.
(2) Roe, R.-J.; Zin, W.-C. *Macromolecules* **1984**, *17*, 189.
(3) Whitmore, M. D.; Noolandi, J. *Macromolecules* **1985**, *18*, 2486.
(4) Winey, K. I.; Thomas, E. L.; Fetters, L. J. *Macromolecules* **1992**, *25*, 2645.
(5) Hashimoto, T.; Koizumi, S.; Hasegawa, H.; Izumitani, T.; Hyde, S. T. *Macromolecules* **1992**, *25*, 1433.
(6) Baek, D. M.; Han, C. D. *Macromolecules* **1992**, *25*, 3706.
(7) Koberstein, J. T.; Russell, T. P.; Pottick, L. *Macromolecules* **1990**, *23*, 877.
(8) Akiyama, M.; Jamieson, A. M. *Polymer* **1992**, *33*, 3582.
(9) Tucker, P. S.; Barlow, J. W.; Paul, D. R. *Macromolecules* **1988**, *21*, 2794.
(10) Tucker, P. S.; Paul, D. R. *Macromolecules* **1988**, *21*, 2801.
(11) Weiss, R. A.; Beretta, C.; Sasonko, S.; Garton, A. *J. Appl. Polym. Sci.* **1990**, *41*, 91.
(12) Lu, X.; Weiss, R. A. *Macromolecules* **1991**, *24*, 4381.
(13) Molnar, A.; Eisenberg, A. *Polym. Commun.* **1991**, *32*, 1001.
(14) Weiss, R. A.; Sen, A.; Willis, C. L.; Pottick, L. A. *Polymer* **1991**, *32*, 1867.
(15) Lu, X.; Weiss, R. A. SPE ANTEC Tech. Pap. **1992**, 1424.
(16) Paul, D.; Barlow, J. W.; Bernstein, R. E.; Wahrmund, D. C. *Polym. Eng. Sci.* **1978**, *18*, 1225.
(17) Kwei, T. K.; Patterson, G. D.; Wang, T. T. *Macromolecules* **1976**, *9*, 780.
(18) Martuscelli, E.; Demma, G. B. In *Polymer Blends*; Plenum Press: New York, 1980.
(19) Keith, H. D.; Padden, F. J., Jr.; Russell, T. P. *Macromolecules* **1989**, *22*, 666.
(20) Zemel, I. S.; Corrigan, J. P.; Woodward, A. E. *J. Polym. Sci.* **1989**, *B27*, 2479.
(21) Gervais, M.; Gallot, B. *Polymer* **1981**, *22*, 1129.
(22) Gervais, M.; Gallot, B. *Makromol. Chem.* **1977**, *178*, 1577.
(23) Nojima, S.; Kato, K.; Yamamoto, S.; Ashida, T. *Macromolecules* **1992**, *25*, 2237.
(24) Makowski, H. S.; Lundberg, R. D.; Singhal, G. H. U.S. Patent 3,870,841, 1975.
(25) Porod, G. *Kolloid Z.* **1951**, 124, 83; **1952**, 125, 51, 108.
(26) Runt, J. P.; Harrison, I. R. *Methods Exp. Phys.* **1980**, *16B*, Chapter 9.
(27) Rim, P. B.; Runt, J. P. *Macromolecules* **1983**, *16*, 762.
(28) Nishi, T.; Wang, T. T. *Macromolecules* **1975**, *8*, 909.
(29) Hoffman, J. D.; Weeks, J. J. *J. Res. Natl. Bur. Stand.* **1962**, *66A*, 13.
(30) Winey, K. I.; Thomas, E. L.; Fetters, L. J. *Macromolecules* **1991**, *24*, 6182.
(31) Weiss, R. A.; Sen, A.; Willis, C. L.; Pottick, L. A. *Polymer* **1991**, *32*, 2785.
(32) Weiss, R. A.; Lefelar, J. A. *Polymer* **1986**, *27*, 3.